



## Designing and manufacturing a portable rainfall simulator

Sima Mohammadi<sup>1\*</sup> , Arian Amini<sup>2</sup> , Amin Salesi<sup>3</sup> , MohammadReza Ahmadi<sup>4</sup> ,  
Mostafa Badiiee<sup>5</sup> , Mahboobe Jalali<sup>6</sup> 

<sup>1</sup> Assistant Professor, Soil Science Department, Lorestan University, Khoramabad, Iran, Email: Simamohammadi.2010@gmail.com

<sup>2</sup> BSc student, Mechanical Engineering Department, Kashan University, Kashan, Iran, Email: Arianamini98@gmail.com

<sup>3</sup> BSc student Mechanical Engineering Department, Kashan University, Kashan, Iran, Email: Aminsalesi1998@gmail.com

<sup>4</sup> BSc student Mechanical Engineering Department, Kashan University, Kashan, Iran, Email: Ahmadimr1377@gmail.com

<sup>5</sup> BSc student Mechanical Engineering Department, Kashan University, Kashan, Iran, Email: Mostafabadiei76@gmail.com

<sup>6</sup> Assistant Professor, Soil Science Department, Lorestan University, Khoramabad, Iran, Email: Mahya\_jalali65@yhoo.com

Article Info	Abstract
<p><b>Article type:</b> Research Article</p> <p><b>Article history:</b> Received: June 2021 Accepted: February 2022</p> <p><b>Corresponding author:</b> Simamohammadi.2010@gmail.com</p> <p><b>Keywords:</b> Drop size distribution Rainfall intensity Rainfall kinetic energy Simulated rainfall Raindrop velocity</p>	<p>Rain simulation is a method widely used in detecting hydrological and erosional processes. Most portable samples are inconvenient and challenging to transport, have high water consumption and energy demand. The objective of this study was to design and test a rainfall simulator characterized by the following innovative features: 1) Easily transported and assembled in the field, thereby allowing the necessary experimental replicates, and 2) Applicability on different slopes. The first calibration step was related to the spatial distribution of rainfall, the stability of the rainfall intensity, and the reproducibility of the rainfall intensities over time (among successive experiments). Next, the drop size distribution (DSD) and the related rainfall characteristics (median volumetric drop diameter D50 and mean kinetic energy per unit area and unit depth) were evaluated by the flour pellet method. A fluorescent tracer method was used to measure the velocity of falling drops. According to the findings, the Christiansen uniformity coefficient (Cu) of the developed rainfall simulator varies from 77-87% for rainfall intensities of 35-75 mmh<sup>-1</sup>. The best rainfall distribution was achieved for rainfall intensities of 55 and 75 mmh<sup>-1</sup>, with rain droplet sizes ranging from 0.6 to 3.8 mm. The raindrop velocity was also measured by photo-shooting and revealed a velocity rate of 2.7-5.7 ms<sup>-1</sup>. The system allows rainfall simulation on the fields and under laboratory conditions. Moreover, using the simulator, erosion, runoff, and sediment production under natural and intact soil conditions can also be examined with the highest possible accuracy.</p>

**Cite this article:** Sima Mohammadi, Arian Amini, Amin Salesi, Mohammadreza Ahmadi, Mostafa Badiiee, Mahboobe Jalali. 2022. Designing and Manufacturing a Portable Rainfall Simulator. *Environmental Resources Research*, 10 (1), 93-104. DOI:10.22069/IJERR.2022.6042



© The Author(s).

DOI: 10.22069/IJERR.2022.6042

Publisher: Gorgan University of Agricultural Sciences and Natural Resources

## Introduction

As production and construction activities are increasing due to the progressive development of global economy, the soil wasting is being accelerated abnormally. Such erosion causes severe land degradation and tension between urban construction and ecological protection (Lv et al., 2019). In this regard, several factors affect the spatial and temporal variability of the land degradation processes. Soil erosion is a widespread environmental problem due to its onsite and offsite adverse impacts. It has been considered one of the significant causes of land degradation globally (Wu et al., 2020). This form of erosion-induced land degradation results in the alteration of soil chemical, mineralogical and physical properties. Understanding the erosion process is crucial for unraveling soil degradation and developing effective land management (Wu et al., 2020).

Previous studies have indicated that soil erosion by water depends on many factors, including slope, rainfall properties (intensity and duration), soil properties, and land management (Shojaei et al., 2020). On the other hand, soil erosion by rainfall includes detachment, transportation, and deposition processes under the combined raindrop effect and overland flow (Wu et al., 2020; Zhang, 2019). Under the impact of raindrops and running water on the surface, soil particles are removed from fertile soil and transported away at a rate that depends on the slope of the land and the amount of runoff (Gao et al., 2020). However, it is difficult to predict and determine the point at which this process is affected by soil or rainfall properties (Shojaei et al., 2020). Knowledge of the rainfall characteristics such as intensity, duration, frequency, and raindrop size distribution and their variation in time and space is essential to conceptualize better a watershed system's hydrological behavior (Abdollahi et al., 2021). To analyze these aspects in more detail, the mass experimental station was recently equipped with a rainfall simulator.

As a practical alternative approach, the rainfall simulator facilitates the quick measurement of different hydrologic

components (Abdollahi et al., 2016). Moreover, it allows the rapid, specific, and replicable assessment of the effect of several factors (e.g., slope, soil type, soil moisture, splash impact of raindrops) on soil loss (Kiani-Harchegani et al., 2018; Mohammadi et al., 2018; Salem et al., 2020). The significant rainfall simulator replicates the natural rainfall process, which is a complex phenomenon and has never been reproduced accurately (Aksoy et al., 2012). Several rainfall simulators have been designed and employed for studies related to soil erosion in the last half-century (Cerdeira, 1997). In most cases, the rainfall simulators employed for field or laboratory experiments are characterized by significant components, limiting the use of the device. Two samples of rain simulator laboratories have been constructed in Iran by the Soil Conservation and Watershed Management Research Institute (Mahmoudabadi et al., 2007) and the Tarbiat Modares University (Abdollahi et al., 2016).

Rainfall simulators on small plots ( $\leq 1$  m<sup>2</sup>) make it possible to distinguish between processes of runoff generation and erosion which leads to presence of an inevitable category (Vergin et al., 2018), for example, the influence of rainfall parameters, different cultivation systems and parameterization of erosion models (Lassu et al., 2015). There are at least four requirements to be met by any portable rainfall simulator: 1) good mobility, 2) easy handling and control of test conditions, 3) homogeneous spatial rainfall distribution, and 4) easy and fast training of operators to obtain reproducible experiments. This list is based on the author's own experience and a review of the relevant literature based on which and the need to distinguish the different partial processes of runoff generation and erosion led to the development of rainfall simulator on small plots (Mhaske et al., 2019).

Generally, rainfall simulators are classified as drop-forming and pressurized nozzle simulators. Regarding the former one, gravity is the leading force for drops; hence, device height is the most crucial factor for the drop velocity to reach the velocity limit, thereby limiting the device's

application. Furthermore, it is challenging to distribute raindrops uniformly across the plot. On the other hand, the raindrops are pressurized in the latter category; hence, the rain is produced at different speeds with uniform distribution depending on the applied pressure.

The two main advantages of rainfall simulators are the accurate control of experiments and precise process measurements (Sadeghi et al., 2013); as such, they are often used in soil erosion studies both in the laboratory and in the field (Vergin, Todisco, & Vinci, 2018). However, calibrated suitable conditions and optimization of the governing situation have been rarely taken into account (Abdollahi et al., 2016). Desirable characteristics for rainfall simulators in hydrological studies include the accurate control of rainfall intensity, the similarity to natural rainfall in terms of kinetic energy, and the spatial rainfall uniformity over the entire test plot. Other important factors include the improved mechanical reliability for easy transportation within research areas (Salem & Meselhy, 2020). The desirable characteristics for rainfall simulators can be evaluated using several techniques such as the staining method (Sadeghi et al., 2013), flour method (Laws & Parsons, 1943; Sadeghi et al., 2013), the photography method (McIsaac, 1990; Sadeghi et al., 2013; Abdollahi et al., 2021) the radar technique (You et al., 2016), and the oil immersion technique (Eigel & Moore, 1983). Most methods are time-consuming and record data temporarily (Sadeghi et al., 2013). They are not applicable anywhere and are too expensive for routine soil erosion studies (Abdollahi et al., 2021). Other researchers have examined uniform rainfall intensity and documented reliable results (Cerdeira & Jurgensen, 2011). To sum up, the accurate evaluation and measurement of rainfall intensity regarding

the nozzle size and hydraulic pressure applied to the nozzle are needed to achieve a maximum resemblance to natural raindrops (Vaezi et al., 2018).

Since the characteristics of different simulators differ depending on the studied climate and research objectives, calibration is needed in other environments according to the regional climatic conditions. Since most studies are conducted in rugged areas with different slopes and sometimes away from residential areas, one of the essential features of simulators is their easy transportation and usability. On the other hand, most simulators that are designed in Iran (Sadeghi et al., 2013) (Kavian et al., 2019) are either fixed or portable without such features. Accordingly, this study aimed to design a rainfall simulator and produce runoff, which was easily transported to different areas and placed on smooth and sloping surfaces, allowing the users to change and control the drop height and water discharge quickly. To make reliable conclusions about the relation between rainfall and soil erosion rates, the characterization of rainfall is indispensable (Cerdeira, 1997; Battany & Grismer, 2000). Therefore, the primary purpose of the following study is to describe the design and set-up of the simulator and the description of the different rainfall parameters of the produced rain.

### **Materials and Methods**

In the present study, a portable rainfall simulator was designed and manufactured to examine hydrological and erosional processes. This simulator was generally intended to be highly mobile on the fields and produce a relatively high rainfall intensity. The experimental structure of the simulator is presented in Figure 1. The simulator's structure and calibration were completed in several steps, as described below.

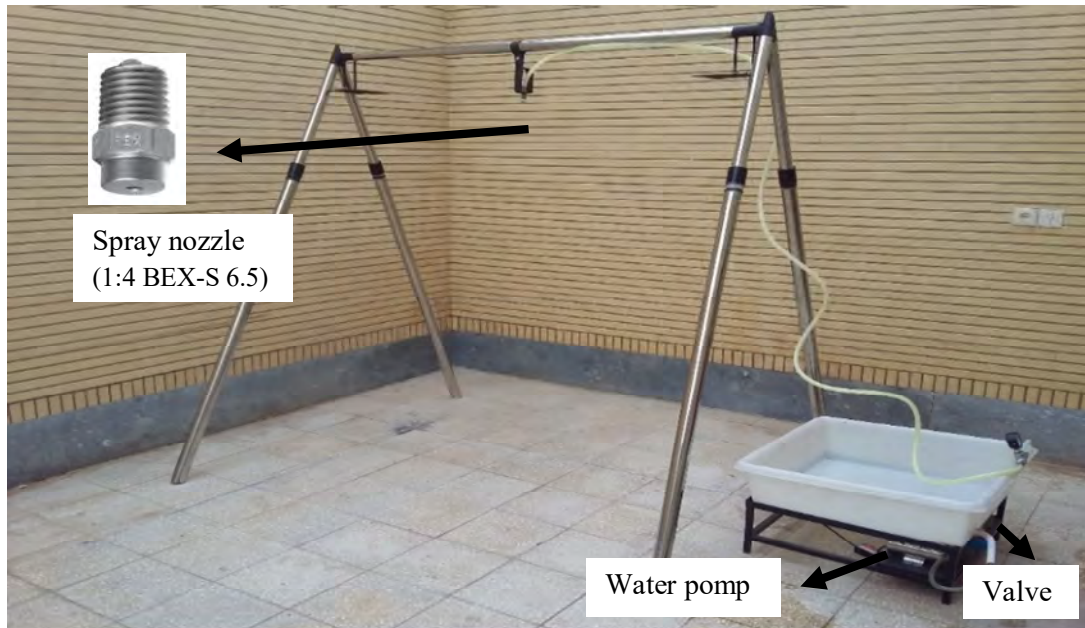


**Figure 1.** Rainfall simulator used for each experimental plot

### **General design of portable rainfall simulator**

The main elements of the rainfall simulator were the frame, spray nozzles, water feeding system, and pressure gauge (Figure 1).

The rainfall simulator developed in this study was designed to be used across a 1 m<sup>2</sup> (1m × 1m) rainfall experimental area. The mainframe was relatively lightweight and portable, and the telescopic legs could increase or decrease the height of the apparatus to adjust stability on rugged terrain. In this device, the nozzle can raise to a maximum height of 2.3 m, allowing the users to perform experiments on slopes up to 30 degrees. In another research, the devices were designed to change the size with no limitation to height holes (Van Dijk et al., 2002). However, the device also had high mechanical strength due to its novel design.

As illustrated in Figure 1, the water feeding system setup encompassed a polyethylene water tank (60 L), a water pump with a maximum power consumption of 90 watts, and a 10-meter head (Yu et al. 2015). The pump drove the rainfall water through the tank's water supply system towards the nozzle. A pipe made of

polyvinyl chloride was used for the whole water supply system, and one control valve was used to control the flow rate and pressure. A pressure gauge at the outlet of the pump was fixed to read the flow pressure.

The single spray nozzle was centrally attached at the top of the structure. The spray nozzle was a 1: 4 BEX- S 6.5 conical bar irrigation nozzle (Figure 1) (Safari et al., 2016) (U.S Patent No. 4,142,682), and the flow rate was controlled by an open/close valve (Figure 1). This nozzle is used successfully in rainfall simulation experiments (Safari et al., 2016), as it provides different rainfall intensities between 35 and 75 mm h<sup>-1</sup> at a pressure between 0.05 to 0.1 MPa.

As shown in Figure 2, the erosion plot consists of 1m×1m galvanized plates attached to the hinge and a trapezoidal plate to lead the plot's runoff and sediment (Kinnell, 2016). To prevent the clean water of nozzle from mixing with the soil runoff under the sample a plate is installed in the trapezoid-shaped plot as a shield which increases the accuracy of the test. The plot's runoff outlet is shot-peened to improve water and soil mixture rate to promote the test precision further.



**Figure 2.** The erosion plot consists of 1m×1m galvanized plates

Wind blow can negatively affect the amount and distribution of precipitation. As a reasonable measure, the equipment is covered with plastic during water applications to reduce the effect of wind on droplet dispersion, thereby promoting the test accuracy regarding the rainfall on the soil.

### Calibration of rainfall simulator

#### *Rainfall Uniformity*

Three rainfall intensities of 35, 55, and 75 mm h<sup>-1</sup> obtained by changing the pump pressure, were selected to calibrate the rainfall simulator. Given the significance of uniformity of raindrop distribution in the simulator, the uniform distribution rate of rain was calculated in three experiments. According to ASTM D6459-15, twenty rainfall containers are required to measure and calibrate rainfall intensity and distribution. In this study, the spatial distribution of the simulated rainfall within the 1 m<sup>2</sup> plot was determined using 20 containers. Each experiment was conducted under the pressures 0.05, 0.06, and 0.08 MPa. The volume of the collected rainfall in each container was measured using a graduated cylinder in (ml), three replicates were undertaken, and the results were converted to intensity values (mm h<sup>-1</sup>). The spatial distribution of the simulated rainfall was displayed using Sigmaplot 12.5 software.

To describe the uniformity of the rainfall events, the Christiansen uniformity

coefficient was used to calculate the raindrop uniform distribution rate (Christiansen, 1942). This coefficient was used to measure the intensity of 20 containers placed on the plot to cover the whole 1×1m plot. The volume of water collected in each container was measured after five minutes of activation, and the uniformity coefficient of rainfall distribution was determined using the following equation (Christiansen, 1942):

$$U = \left[ 1 - \frac{\sum_{i=1}^n |M_i - A|}{n * A} \right] \times 100 \quad [1]$$

where U is the uniformity coefficient, M is the measured water from the containers (cm), A is the mean water measured (cm), and n is the number of containers (n=20 in this study).

#### *Raindrop size distribution*

The raindrop size distribution was determined to assess potential erosion at the soil surface (Lora et al., 2016), and the flour pellet method was used to calculate the raindrop size (Hudson, 1963). For each intensity, the raindrops were allowed to fall into a deep layer of fine flour. The plate was kept above the soil surface (about 10 cm above the soil surface) and exposed to rain for 3 seconds (when the rainfall intensity was fixed) (Laws & Parsons, 1943). As soon as the raindrops fell on the flour, they created small pellets on the surface flour. Then the plate flour was dried for 24 h to harden the pellets (Sadeghi et al., 2013). An image of each plate was then

achieved by scanning and evaluated by an image analysis software (i.e., Digimizer) to calculate their diameters. In this software, the droplet diameters can be easily measured by defining an index, as presented in Figure 3. This method was

replicated more than four times for each intensity. In other words, the raindrop size was evaluated by detecting and analyzing more than 100 drops for each pressure. It seems reasonable to assume that raindrop is perfectly spherical (Cruvinel et al., 1999).

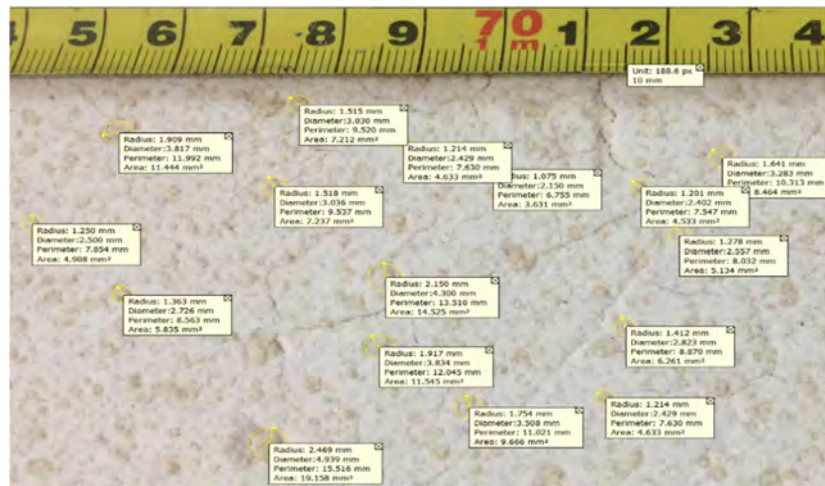


Figure 3. Calculation of simulated raindrop diameters by Digimizer software

### Raindrop velocity

The test method dissolved about 100 grams of fluorescent dye in tank water (30 L). The amount of dissolved dye was sufficient while not changing the water's physical properties and droplet velocity (Lepmert et al., 1995). When the device was turned on

and achieved a steady state after a few seconds, using a 240-fps video camera, the droplets were filmed in a dark room in front of a UV-A light projector, making the droplets glow in the dark. Figure 4a illustrates this experimental procedure.

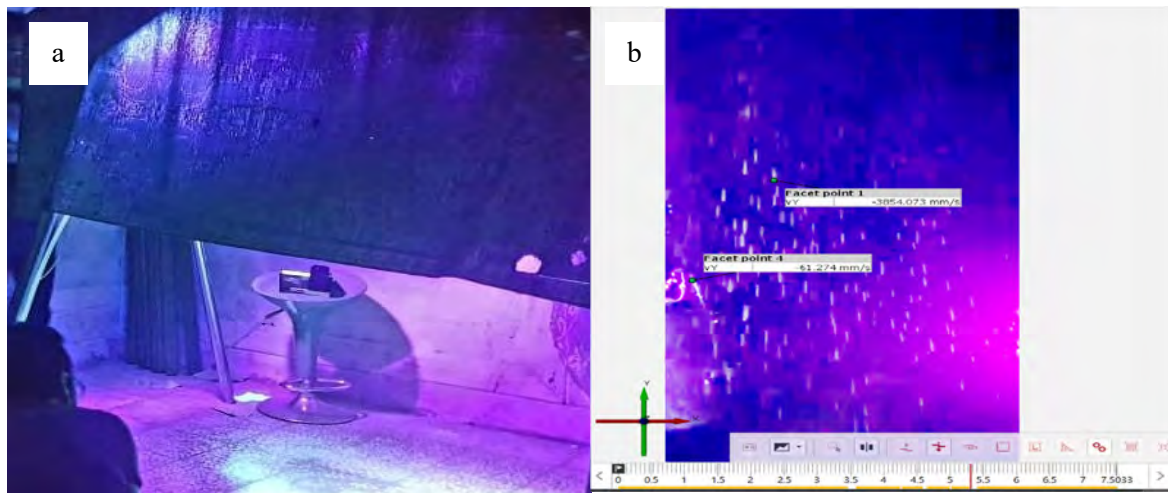


Figure 4: a) Raindrop velocity test setup, b) GOM correlate software result

The diameter and fall speed of the raindrops were measured using a slow-motion video, and the velocity of 10 droplets was then measured randomly. The

videos recorded from the droplets were analyzed using “GOM correlate” software (Lepmert et al., 1995).

The image processing method was to insert the video into the software, define a part of the previously-measured imaging location as an index in the software, select a fixed reference point and desired droplets, and ultimately process them. The fixed-point speed is evaluated with the completion of video processing by the software, which must be about zero concerning the error. Finally, the droplet velocities are saved (Figure 4 b).

### **Kinetic energy**

To understand the rainfall erosion index, the rainfall kinetic energy (KE) should be calculated. The rainfall kinetic energy is an efficient index affecting the potential ability of the rainfall in separating soil particles from the soil surface. The rainfall distribution can calculate the KE and velocity of raindrops. Accordingly, the kinetic energy rate per unit rainfall during an event (in  $J m^{-2}mm^{-1}$ ) is usually determined.

In this study, the kinetic energy of the simulated rainfall was determined using the raindrop size distribution and its velocity. The KE of a droplet is calculated based on the following equation (Salles et al., 2002):

$$KE = \sum \frac{1}{2} MV^2 = \sum \frac{1}{12} \pi \rho D^3 V^2 \quad [2]$$

where  $M$  is the mass of the droplet (kg),  $V$  is the velocity ( $m s^{-1}$ ),  $\rho$  is the density of water ( $kg m^{-3}$ ), and  $D$  is the diameter of a raindrop (m).

### **Results and Discussion**

Calibration experiments were performed to quantify the performance of the rainfall simulator and determine whether the device could consistently simulate rainfall with features similar to natural rainfall. The results of the present study are as follows.

#### **Raindrop size distribution**

Natural rainfall contains a wide distribution of drop sizes varying from near 0.1 mm to about 7 mm in diameter (high-intensity rain) (Fernandez-Galvez et al., 2008). Table 1 lists the drop size distribution for each rainfall intensity. The histograms of the drop size distribution for the three rainfall intensities are presented in Figure 5. The diameter of the rain droplets ranges from about 0.6 mm to 3.8 mm, and the maximum number of drops occur for the diameter range of 1.4-1.6 mm for 35  $mm h^{-1}$  and 1-1.2 mm for 55 and 75  $mm h^{-1}$  rainfall intensities.

**Table 1.** Raindrop-size distribution at 35, 55 and 75  $mm h^{-1}$  intensity

	Diameter of the rain droplet (mm)	Rainfall intensity ( $mm h^{-1}$ )		
		35	55	75
		Number of drops		
1	<0.6	4	1	4
2	0.6-0.8	3	4	4
3	0.8-1	4	5	10
4	1-1.2	10	22	30
5	1.2-1.4	12	18	17
6	1.4-1.6	16	15	10
7	1.6-1.8	11	10	6
8	1.8-2	8	6	5
9	2-2.2	6	3	4
10	2.2-2.4	5	4	3
11	2.4-2.6	4	3	2
12	2.6-2.8	3	3	1
13	2.8-3	4	2	2
14	3-3.2	2	2	1
15	3.2-3.4	2	1	1
16	3.4-3.6	4	1	0
17	3.6-3.8	2	0	0
18	3.8<	0	0	0

In the raindrop size measurement using the flour pellet method, the raindrop was assumed to be perfectly spherical.

Concerning the raindrop size distribution in Figure 8, the rainfall simulator could produce different diameters as the rainfall

intensity could vary. The findings indicate that the median raindrop diameter ranged

from 1.4 to 1.6 at 35 mm h<sup>-1</sup> and from 1 to 1.2 mm at 55 and 75 mm h<sup>-1</sup>.

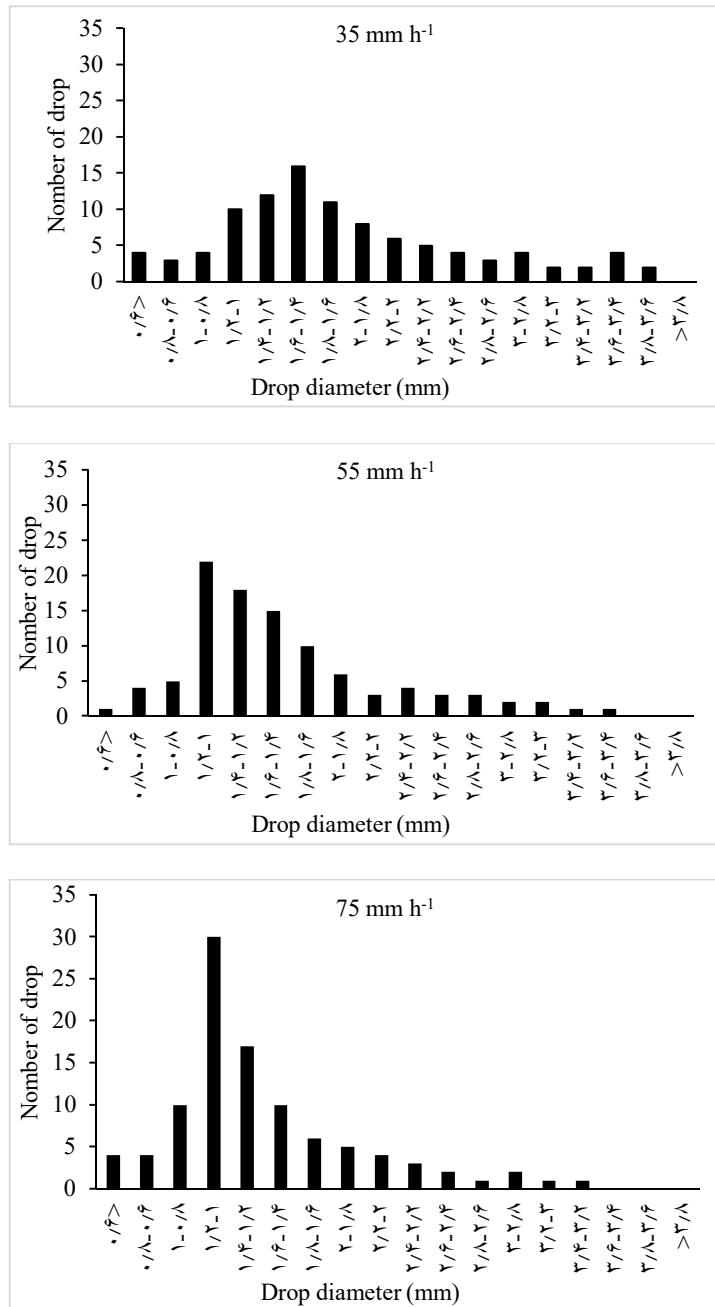


Figure 5. Drop size distribution of the rain droplets for 35, 55, and 75 mm h<sup>-1</sup> rainfall intensities.

The observation confirms the relationship between the applied rainfall intensity and the raindrop size, in which, with increasing the rainfall intensity, the diameter of the simulated raindrops decreases.

The median diameters (D<sub>50</sub>) were equal to 1.5, 1.3, and 1.2 for the 35, 55, and 75 mm h<sup>-1</sup> rainfall intensities, while most raindrops were between 1 and 2 mm.

Similar measurements were declared by Abudi et al. (2012), with a mean raindrop diameter of 1.5 mm. Salem et al. (2020) also reported that the drop diameter of simulated rainfall varied from 0.8 mm to about 2.1 mm for the 14 and 80 mm h<sup>-1</sup> rainfall intensities, respectively. In this study, the mean diameter of raindrops was smaller than the values reported in other



studies. For example, the median raindrop diameter obtained by Kato et al. (2009) was 3.5 mm at 170 mm h<sup>-1</sup> rainfall intensities. Also, Kavian et al. (2018) reported drop diameters of 0.8 to 2.4 mm at 20 to 80 kPa, it ranged from 1 to 1.2 mm at 20 and 40 kPa, and from 0.4 to 0.6 mm at 80 kPa. Few large raindrops (> 3mm) were reached only at the pressure 0.05 MPa. The maximum raindrop size decreases continuously with increasing rainfall intensity.

Simulating rainfall with an intensity of 57.1 mm/h, Cerda et al. (1997) reported a median drop size of 2.49 mm. Kavian et al. (2018), using a 2-nozzled rainfall simulator, also showed rains with mid-diameter raindrops of about 0.8 to 2.4 mm for different intensities. Compared to other tests in terms of droplet size, it can be noticed that the droplet size is similar to natural rain and cover a wide range of different droplet sizes (Loch and Foley, 1994; Cerda, 1997; Sadeghi et al. 2013; Kinnell, 2016; Kavian et al. 2018). Sadeghi et al. (2013) measured a natural rain droplet size of 0.2 to 5.16 mm using the imaging method. They stated that the median diameter of raindrops was scattered at intensities ranging from 0.6 to 1.5 mm. As discussed in many research types, the raindrop diameters of natural rain

are not uniform; hence, producing non-uniform raindrops is necessary for bringing rain simulations closer to natural rainfall (Lassu et al., 2015). The consistency of the drop-size in an experimental distribution influences the hydrological and sedimentological response of soil surfaces significantly (Bowyer-Bower & Burt, 1989).

### **Raindrop velocity**

Table 2 summarizes the fall velocity of raindrops at different pressures ranging from 3.5 to 5.7 m s<sup>-1</sup>. The raindrop velocity is associated with the raindrop size due to the relationship between the raindrops and the rainfall intensity; as such, the raindrop velocity is dependent on the rainfall intensity. As shown in Table 2, the fall velocities were 3.5, 4.8, and 5.7 m s<sup>-1</sup> for the rainfall intensity of 35, 55, and 75 mm h<sup>-1</sup>, respectively. This finding agrees with that of Kavian et al. (2018), as the fall velocity was 5.1 ms<sup>-1</sup> for the rainfall size of 2- 2.5 mm. Abudi et al. (2012) estimated the drop velocity of 2.5-5.7 m s<sup>-1</sup> for the raindrop of 0.8 to 5 mm. Salem et al. (2020) indicated that the terminal rates ranged from 3.35 to 5.64 m s<sup>-1</sup> for the intensities of 14 and 45 mm h<sup>-1</sup>.

**Table 2.** Rainfall intensities, coefficient of Christiansen Uniformity (CU) and Velocity at different pressures

Pressure (MPa)	Rainfall intensity (mm h <sup>-1</sup> )	CU (%)	Median diameter D50 (mm)	Velocity (m s <sup>-1</sup> )
0.05	35	77	1.5	3.5
0.06	55	85	1.3	4.8
0.08	75	87	1.2	5.7

### **Uniformity of rainfall distribution**

Figure 6 shows the rainfall distribution of each experimental plot at the three pressures. According to this figure, the coefficient of Christiansen uniformity (CU) ranged from 77 to 87%. These CU values are comparable to those obtained in many studies. For example, Clarke and Walsh (2007) produced a CU of 88%. Alves Sobrinho et al. (2008) achieved CUs of 81.4 - 85.1%, and Mhaske et al. (2019) reported a CU of 81-88%. The distribution of rainfall intensity across a container placed on the plot was relatively uniform. However, rainfall intensity was uniform

over the entire container and did not remarkably vary between the rain simulation units.

The results further indicated that the uniformity coefficient was 77, 85, and 87% for the intensities of 35, 55, and 75 mm h<sup>-1</sup>, respectively. As shown in Table 2, when the simulated rainfall intensity increases, the uniformity coefficient increases. When the intensity increased from 35 to 75 mh<sup>-1</sup>, the uniformity coefficient increased from 77 to 87%. The rainfall can be considered uniform when CU is >80% (Moazed et al., 2010). However, the spatial rainfall distribution under rainfall intensity of 35

exhibits a concentric pattern with the highest amount of rainfall recorded in the center and the lowest amount of rainfall recorded around the plot rim (Figure 6). The water pressure system was decreased as much as possible to reach the most significant drop size. This reduces the

amount of heterogeneity of spatial distribution across the plot under low intensity rainfall. In contrast, the heterogeneity decreased with increasing rainfall intensities. This finding shows that the uniformity coefficient is sensibility affected by the rainfall intensity.

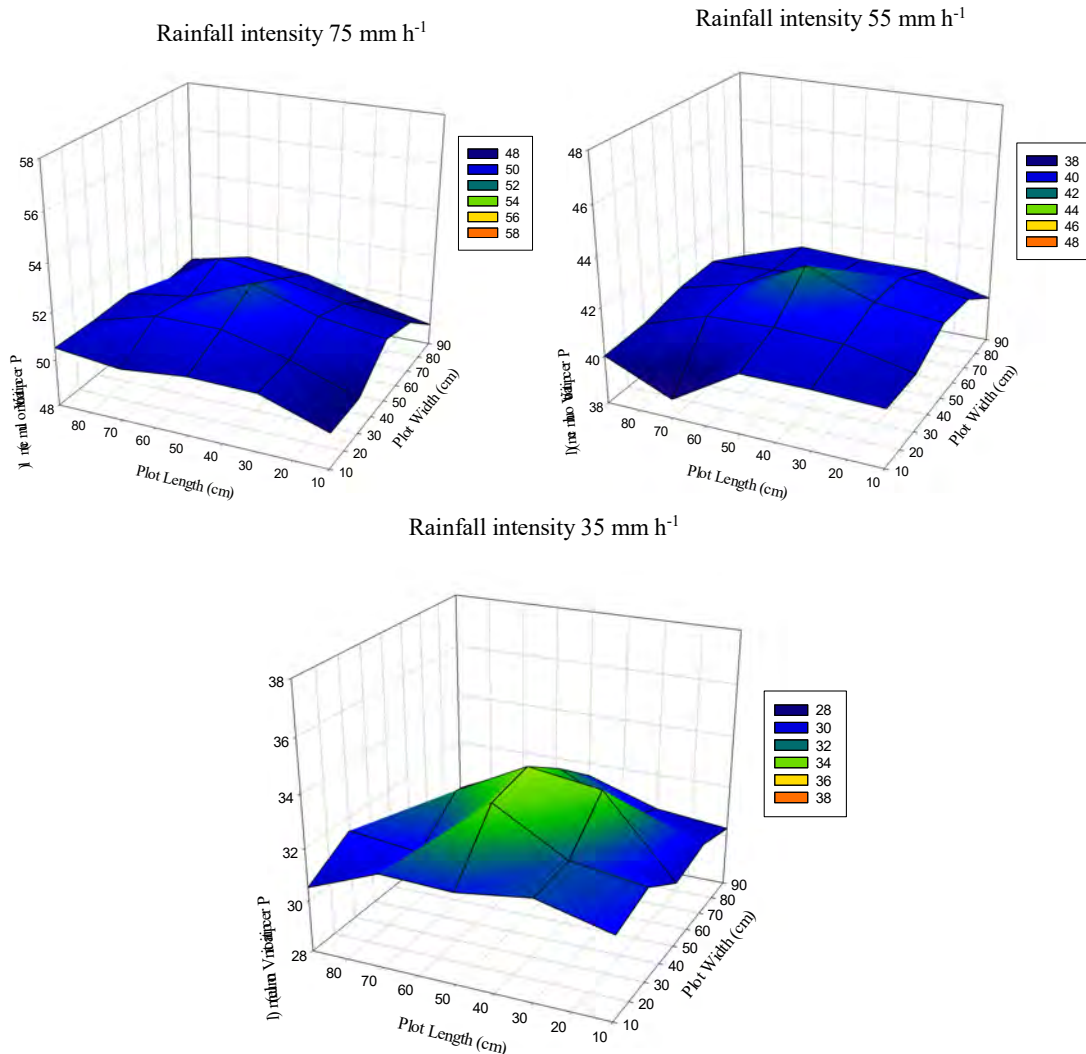


**Figure 6.** Spatial rainfall intensity distribution (for three intensities 35, 55, and 75 mm h<sup>-1</sup>)

### ***Kinetic energy***

A 55 mmh<sup>-1</sup> rainfall produced by the simulator was estimated to have a KE rate per unit time of 20.5 J m<sup>-2</sup> mm<sup>-1</sup> using the drop-size distribution and impact velocities which are measured in preceding sections. The smaller drops (<1 mm diameter) generate only 1 % of the total rainfall KE since they represent a much smaller mass. The raindrops of 1-3 mm diameter mainly produce KE due to their magnitude and

comparative frequency. The simulator's higher KE rate reflects that the extremely high rainfall intensity outweighs the impacts of velocities. Furthermore, Salem et al. (2020) reported the kinetic energy of raindrops to be in the range of 12.7-18.9 J m<sup>-2</sup> mm<sup>-1</sup>. The detection of the relationship between kinetic energy and rainfall intensity is necessary for predicting soil loss risk.

## Conclusion

A portable rainfall simulator designed, manufactured, constructed, and calibrated for laboratory and field research. The simulator is easy to transport and use in remote locations; it was manufactured at a low cost, before starting each experiment. The simulator, however requires calibration based on the properties of regional precipitation. The rainfall simulator can produce rainfall intensity ranging from 35 to 75 mmh<sup>-1</sup> over a 1 m<sup>2</sup> plot. The simulator can simulate precipitation with a raindrop diameter range of 0.6 to 3.8 mm, and a

Christiansen uniformity coefficient of 77 to 87%, which indicates a highly uniform distribution. The results also show that the fall velocity of raindrops ranged between 3.5 to 5.7 mms<sup>-1</sup>. The current design permits flexibility in both droplet diameter and rainfall intensity. The device optimizations made rainfall simulation and runoff production possible in diverse areas with easier transportation and more accurate applications. In the future, it is proposed to control runoff output for rainfall simulators to enhance its many advantages.

## References

- Bowyer-Bower, T.A., and Burt, T.P. 1989. Rainfall simulators for investigating soil response to rainfall. *Soil Technology*. 1-16.
- Cerda, A., and Jurgensen, M. 2011. Ant mounds as a source of sediment on citrus orchard plantations in eastern Spain. A three-scale rainfall simulation approach. *Catena*. 231-236.
- Cerda, A., Ackermann, O., Terol, E., and Rodrigo-Comino, J. 2019. Impact of farmland abandonment on water resources and soil conservation in citrus plantations in Eastern Spain. *Water*. 824.
- Cerda, A. 1997. Rainfall drop size distribution in the Western Mediterranean basin, Valencia Spain. *Catena*. 30 (2-3), 169-182.
- Christiansen, J.E. 1942. Irrigation by sprinkling. California: University of California Agricultural Experiment Station Bulletin .
- Clarke, M., and Walsh, R.P. 2007. A portable rainfall simulator for field assessment of splash and slopewash in remote locations. *Earth Surface Processes and Landforms*. 2052-2069.
- Cruvinel, P., Vieira, S.R., Crestana, S., Minatel, E.R., Mucheroni, M.L., and Neto, A.T. 1999. Image processing in automated measurements of raindrop size and distribution. *Computers and Electronics in Agriculture*. 205-217.
- Eigel, J., and Moore, I. 1983. A simplified technique for measuring raindrop size and distribution . *Transactions of the American Society of Agricultural Engineers*. 1079-1084.
- Fernandez-Galvez, J., Barahone, E., and Mingorance, M. D. 2008. Measurement of infiltration in small field plots by a portable rainfall simulator: Application to Trace-Element mobility. *Water Air Soil Pollution*. 257-264.
- Gao, L., Bowker, M., Sun, H., Zhao, J., and Zhao, Y. 2020. Linkages between biocrust development and water erosion and implications for erosion model implementation. *Geoderma*. 113973.
- Hudson, N. 1963. Raindrop size distribution in high intensity storms. *Rhodesian Journal of Agricultural Research*. 1-16.
- Kato, H., Onda, Y., Tanaka, Y., and Asano, M. 2009. Field measurement of infiltration rate using an oscillating nozzle rainfall simulator in the cold, semiarid grassland of Mongolia. *Catena*. 173-181.
- Kavian, A., Gholami, L., and Mohammadi, M. 2018. Impact of Wheat Residue on Soil Erosion Processes. *Notulae Botanica Horti Agrobotanici Cluj-Napoca*. 553-562.
- Kavian, A., Mohammadi, M., Cerda, A., Fallah, M., and Gholami, L. 2019. Design, manufacture and calibration of the SARI portable rainfall simulator for field and laboratory experiments. *Hydrological Sciences Journal*. 350-360.
- Kinnell, P. I. 2016. A review of the design and operation of runoff and soil loss plots. *Catena*. 257-265.

- Lassu, T., Seeger, M., Peters, P., and Keesstra, S.D. 2015. The Wageningen rainfall simulator: set-up and calibration of an indoor nozzle-type rainfall simulator for soil erosion studies. *Land Degradation and Development*. 604-612.
- Laws, J. O., and Parsons, D. A. 1943. The relation of raindrop size to intensity. *Proceedings of the 24th Annual Meeting Transactions of American Geophysical Union*, (pp. 452-460).
- Lepmert, W., Magee, K., Ronney, P., Gee, K., and Haugland, R. 1995. Flow tagging velocimetry in incompressible flow using photo-activated noninvasive tracking of molecular motion (PHANTOMM). *Experimental in Fluids*. 249-257.
- Loch, R., and Foley, J. 1994. Measurement of aggregate breakdown under rain comparison with tests of water stability and relationships with field measurements of infiltration. *Soil Research*. 701-720.
- Lora, M., Camporese, M., and Salandin, P. 2016. Design and performance of a nozzle type rainfall simulator for landslide triggering experiments. *Catena*. 77-89.
- Lv, J., Luo, H., and Xie, Y. 2019. Effects of rock fragment content, size and cover on soil erosion dynamics of spoil heaps through multiple rainfall events. *Catena*, 179-189.
- Mahmoodabadi, M., Rouhipour, H., Asadi, H., and Iranajad, M. 2007. Intensity calibration of SCWMRI rainfall and erosion simulator, *Journal of Watershed Management Science Engineering*. 39-50.
- McIsaac, G. 1990. Apparent geographic and atmospheric influences on raindrop sizes and rainfall kinetic energy. *Journal Soil Water Conservation*. 663-666.
- Mhaske, S.N., Pathak, K., and Basak, A. 2019. A comprehensive design of rainfall simulator for the assessment of soil erosion in the laboratory. *Catena*. 408-420.
- Moazed, H., Bavi, A., Boroomand-Nasab, S., Naseri, A., and Albaji, M. 2010. Effects of climatic and hydraulic parameters on water uniformity coefficient in solid set systems. *Journal Applied Science*. 1792-1796.
- Mohammadi, S., Homaei, M., and Sadeghi, S.H. 2018. Runoff and sediment behavior from soil plots contaminated with kerosene and gasoil. *Soil and Tillage Research*. 1-9.
- Sadeghi, S.H., Abdollahi, Z., and Darvishan, A. 2013. Experimental comparison of some techniques for estimating natural raindrop size distribution on the south coast of the Caspian sea, Iran. *Hydrology Sciences Journal*. 1382-1374.
- Safari, A., Kaviani, A., Parsakhoo, A., Saleh, I., and Jordan, A. 2016. Impact of different parts of kids trails on runoff and soil erosion in the Hyrcanian forest (northern Iran). *Geoderma*. 161-167.
- Salem, H., and Meselhy, A. 2020. A portable rainfall simulator to evaluate the factors affecting soil erosion in the northwestern coastal zone of Egypt. *Natural Hazards*. 20-40.
- Shojaei, S., Kalantar, Z., and Rodrigo-Comino, J. 2020. Prediction of factors affecting activation of soil erosion by mathematical modeling at pedon scale under laboratory conditions. *Scientific Reports*. 1-11.
- Vaezi, A., Eslami, S., and Keesstra, S. 2018. Interrill erodibility in relation to aggregate size class in a semi-arid soil under simulated rainfalls. *Catena*. 385-398.
- Van Dijk, A., Bruijnzeel, L., and Rosewell, C. 2002. Rainfall intensity-kinetic energy relationships: a critical literature appraisal. *Journal of Hydrology*. 1-23.
- Vergin, L., Todisco, F., and Vinci, A. 2018. Setup and calibration of rainfall simulator of the Mass experimental station for soil erosion studies. *Catena*. 448-455.
- Wu, X., Wei, Y., Cai, C., Yuan, Z., Liao, Y., and Li, D. 2020. Effect of erosion-induced land degradation on effective sediment size characteristics in sheet erosion. *Catena*. 1-15.
- You, C., Lee, D., Kang, M., and Kim, H. 2016. Classification of rain types using drop size distribution and polarimetric radar: case study of a 2014-flooding event in Korea. *Atmospheric Research*. 211-219.
- Yu, J., Yu, H., and Huang, X. 2015. Mobilization and distribution of lead originating from roof dust and wet deposition in a roof runoff system. *Environment Science Pollution Research Int.* 40-50.
- Zhang, X. 2019. Determining and modeling dominant processes of interrill soil erosion. *Water Resource Research*. 4-20